Geochemical characteristics of Holocene sediments from Chuadanga district, Bangladesh: Implications for weathering, climate, redox conditions, provenance and tectonic setting

Ismail Hossain[1*], Krisna Kanta Roy[1], Pradip Kumar Biswas[2], Mahbubul Alam[3], Md. Moniruzzaman[4], and Farah Deeba[4]

[1] Department of Geology and Mining, University of Rajshahi, Bangladesh

[2] Institute of Mining, Mineralogy and Metallurgy (IMMM), Joypurhat, Bangladesh

[3] Water Resource Planning Division, Institute of Water Modelling (IWM), Dhaka, Bangladesh

[4] Institute of Nuclear Science and Technology (INST), Atomic Energy Commission, Dhaka, Bangladesh

[*] Corresponding author, E-mail: ismail_gm@ru.ac.bd

Abstract   The present research deals with the geochemical characteristics of the Holocene sediments from Alamdanga area, Chuadanga district, Bangladesh. Main goals of the study are to delineate source rock characteristics, degree of chemical weathering and sorting processes and behavior of redox conditions during deposition of the sediments. Geochemical characteristics of the sediments show comparatively a wide variation in accordance with stratigraphy in their major element contents (e.g. SiO_2 69.46–82.13, Al_2O_3 2.28–8.88 in wt%), reflecting the distinctive provenance and in part an unstable period in terms of tectonic activity. Geochemical classification of the sediments shows mostly sub-arkose with few sub-litharenites. Some major and trace elements display comprehensible correlation with Al_2O_3 confirming their possible hydraulic fractionation. The chemical index of alteration (CIA*), W* index, index of compositional variability (ICV), plagioclase index of alteration (PIA*) values and the ratio of SiO_2/Al_2O_3, suggest low degrees of chemical weathering in the source areas as well as immature to moderately mature the sediments. The sediments suggest semi-arid climatic trends within oxic deltaic depositional conditions during the Holocene, at 3–12 ka. Whole rock geochemistry and discrimination diagrams demonstrate the continental signature derivatives, which might have been derived from the felsic to intermediate igneous rocks (granitic plutonic rocks) as well as from quartzose sedimentary/metamorphic provenance. These typical sources are present in a vast region of the Himalayan belt and catchment areas of Ganges. The tectonic setting of the sediments demarcates typically passive margin with slightly continental arc system.

Key words   chemical index of alteration; W* index; compositional variability; oxic condition; deltaic deposit; passive margin

1 Introduction

The Himalayan orogenic belt is one of the largest collision orogens in the world, which separates the Eurasia with Burmese sub-plate from Indian subcontinent, Iran, Nubian-Arabia sub-plate in the south. Accurate knowledge of the structure and history of this orogenic belt has played a crucial part in understanding the tectonic evolution of the Indian subcontinent, especially the Bengal Basin, a deepest sedimentary basin of the world (Curray and Moore, 1971). Accordingly, the Bengal basin is an ideal location to observe the tectonic uplift and erosion history of the Himalaya, and also paleo-weathering. It is well established that chemical weathering in the Himalaya and global climate have potential correlation and Himalayan uplift also is the dominant driver for Miocene global climate (Raymo and Ruddiman, 1992). The study area is within the Faridpur trough of Bengal foredeep located in the western part of the Bengal basin and one of the significant domains of Ganges-Brahmaputra (G-B) delta. It is assumed that sediment budgets of the Faridpur trough are mainly from Himalayan orogens with some shear of Indian cratonic

contributions. Generally lithified sediments provide decisive information for provenance studies, and for reconstructing the tectonic, climate, and geographic setting of sedimentary basins (Basu, 1985). The studied Holocene sediments provide available information for source rock characteristics, with relief and climate, transport and depositional mechanisms (Dickinson et al., 1983; Basu, 1985; Dickinson, 1985). So, the geochemistry of clastic sediments is the product of interacting factors including provenance, sorting, weathering and tectonism (Johnsson, 1993; McLennan et al., 1993). On these contexts a number of geochemical studies on draining sediments of Himalaya (Dalai et al., 2004; Sinha et al., 2007; Najman et al., 2008; Hossain et al., 2010; Roy and Roser, 2012) have been carried out and provided some valuable information on the depositional history of this region. In detailed geochemical study of Holocene sediments from Chuadanga area, Bangladesh is still lacking, though these clastic sediments put up with a great tectonic significance. So, the present work has designed to use geochemical composition of core sediments for delineating sediment types, weathering, climate, redox conditions, provenance of sediments, and tectonic setting of the Bengal Basin. This research work will help in understanding the geochemical evolution of the Faridpur trough sediments during Holocene time and control of provenance, weathering and sediment routing in the G-B delta and thus contribute to basin-wide regional correlation.

2 Geological setting

The Bengal Basin is an asymmetric basin with a huge thickness of sediments that increases toward the southeast (Curray and Moore, 1971). The dynamic nature of the basin can be attributed to the interaction of three plates, namely the Indian, Eurasian and Burmese (West Burma Block) Plates. The geological history of the basin is related to the rifting and separation of the Indian Plate from the combined Antarctica-Australia part of the Gondwana and it spectacular journey, initially northwestward and then northward (Uddin and Lundberg, 2004). During the initial phase of the basin development the plate was moving towards north and rotating anticlockwise. The initial collision with the Burmese Plate, probably during the Late Eocene, resulted in rising of an Eocene island arc. This event created two basins, the Irrawady Basin in the east and to the west the Bengal Basin. Both basins were connected with the Tethys Ocean in the northwest. During the Miocene the Tethys was separated from these two basins. The Bengal Basin and the Irrawady Basin were separated from each other during the Miocene. From then onward due to subduction of the Indian Plate beneath the Burmese Plate and anti-

clockwise rotation, the basin started closing in the northeast and gradually turned into a remnant basin (Uddin and Lundberg, 2004). According to a recent study by Najman et al. (2008), Himalayan sediments started to deposit in the Bengal Basin during the Eocene, at ~38 Ma. The investigated sedimentary sequence in the borehole belongs to the Holocene in age within one of the world's largest G-B delta (Stanley and Hait, 2000). During this period, an estimated seaward-directed suspended sediment load of 1060×10^6 t/a (Milliman and Syvitski, 1992) have been deposited in the floodplain and coastal areas of the Bengal Basin in response to the Himalayan upliftment, climatic change and fluctuations in sea level during the Late Pleistocene and the Holocene. These suspended sediments deposited in the Ganges-Brahmaputra deltaic conditions probably during the Holocene, at ~3–12 k ages (Stanley and Hait, 2000). During this period, Holocene mean sedimentation rate was estimated about <0.7 cm/a, which was comparable to modern depositional rates seaward of the coast. These seaward depositional rates confirm that there has been active seaward progradation of the sub-aqueous delta in recent time (Allison, 1998). Over the last decade extensive works have been carried out in the delta formed by Ganges-Brahmaputra rivers of India and Bangladesh (Stanley and Hait, 2000; Sarkar et al., 2009; Pate et al., 2009). These studies revealed important information on the evolution of the Bengal Basin and the changes in sediment budgets/dispersal through time and space (Allison et al., 1998, 2003).

Geographically the study area falls in the Alamdanga Upazila under Chuadanga district of Bangladesh. The borehole position is about latitude 23°45.706′N and longitude 88°56.762′E (Fig. 1a). The study area lies in the Faridpur trough of Bengal foredeep, which is nearly the Hinge zone in the west and Barisal-Faridpur uplift in the east. Faridpur trough is characterized by a general gravity low of northeast trend which is apparently related to general subsidence of basement (Khan, 1991). The sedimentary sequence of the borehole contains repeated grey to light grey, coarse to fine grained sediments, except depth 86–105 m contain light grey gravely sand and some places fine sand to silt deposits (Fig. 1b).

3 Materials and methods

The composite samples from considerable depths (Fig. 1a) were collected from the borehole (~137 m in depth) and preserved in the polyethylene bags. Collected raw and wet samples were dried up primarily by natural sunlight. Although a total of 44 samples were collected, only 12 samples (Fig. 1a) were analyzed using X-ray Fluorescence Spectrometer (XRF).

Each sample was crushed for 20 minutes in a planetary ball mill (PM-200, Retsch, Germany) to make powder form in well mixing conditions. The powder samples were then pulverized in a pulverizer machine. The dried powder samples were mixed with binder (stearic acid: sample at a ratio of 1:10) and pulverized for two minutes. The resulting mixture was spooned into an aluminum cap (30 mm). The cap was sandwiched between two tungsten carbide pellets using a manual hydraulic press with 10–15 ton/sq.in. for 2 minutes and finally pressure was released slowly. The pellet was then ready for X-ray analysis. The elements were determined by X-ray fluorescence (XRF) spectrometer method at Institute of Mining, Mineralogy and Metallurgy, Joypurhat following the procedures of Goto and Tatsumi (1994, 1996) using Rigaku ZSX Primus XRF machine equipped with an end window 4 kW Rh-anode X-ray tube. The heavy and light elements were determined using 40 kV voltage with 60 mA current respectively. The standards used in the analyses are the Geological Survey of Japan (GSJ) Stream Sediments and USGS Rock Standards. Analytical uncertainties for XRF major and minor elements are ~2% and trace elements are <10%.

From geochemical data (Table 1), different indices and diagrams are calculated/prepared using major oxides. For MFW ternary plot, formulas for calculating vertices are followed Ohta and Arai (2007) and W vertex is also used to calculate W* index, there CaO* represents the CaO in the silicate fraction only. Whereas, $ICV = [Fe_2O_3 + K_2O + Na_2O + CaO + MgO + TiO_2/Al_2O_3]$, $IA* = [100 \times *][Al_2O_3/(Al_2O_3 + CaO* + Na_2O + K_2O)]$ and $PIA* = [(Al_2O_3 - K_2O)/(Al_2O_3 + CaO* + Na_2O - K_2O)] \times 100$, there CaO* represents also the CaO in the silicate fraction only (Fedo et al., 1995). It is note that CO_2 data of the present study are not available. In this case, the data have been corrected based on the methods of McLennan (1993). The content of CaO corrected for apatite using P_2O_5 ($CaO* = CaO - (10/3 \cdot P_2O_5)$). If the corrected CaO^* was lower than the amount of Na_2O, this corrected CaO* value adopted. In this regard, if the CaO* value is higher than the amount of Na_2O, it was assumed that the correction of CaO equal that of Na_2O.
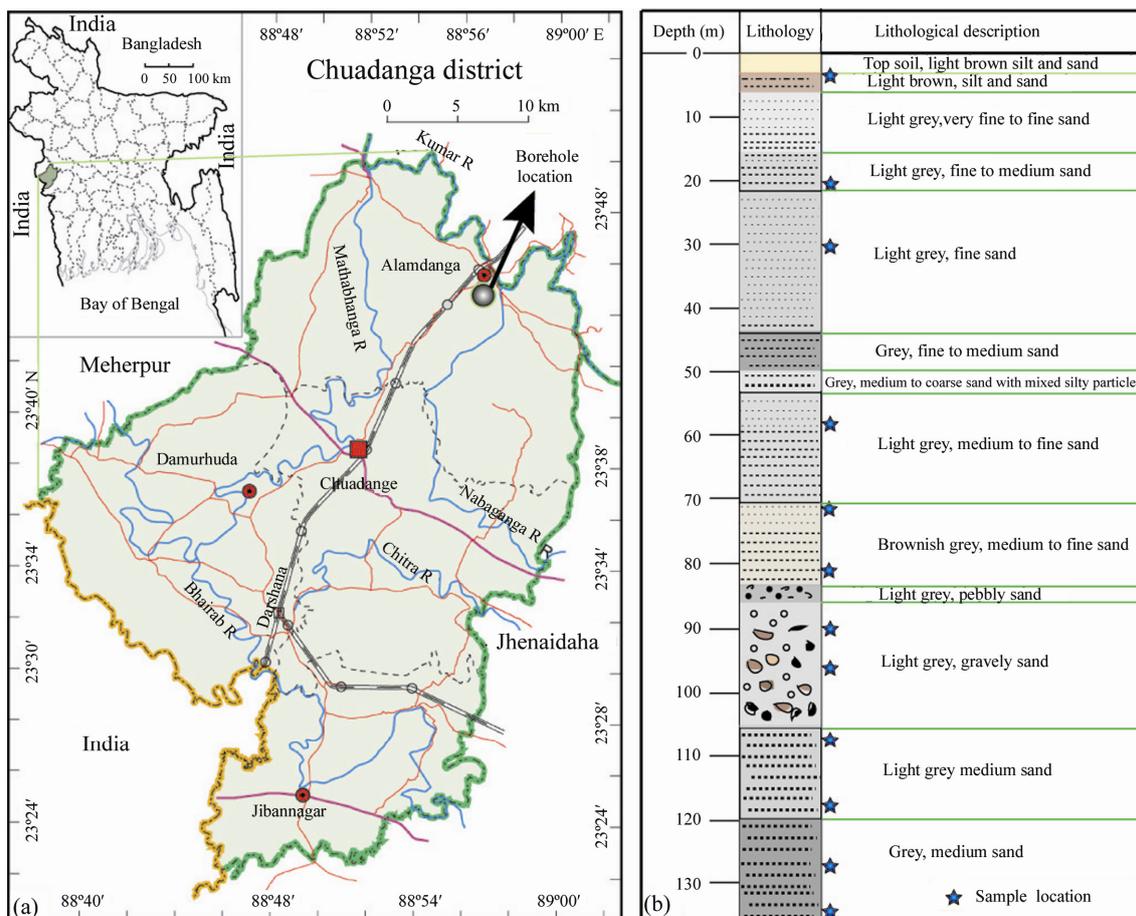

Fig. 1. (a) Location map of the study area showing borehole position; (b) horehole, sample locations and lithological descriptions.

Table 1   Major and trace elemental abundances and CIA*, PIA*, W*, ICV, Mn* values of the investigated Holocene sediments

Oxide (wt%)	A-01	A-07	A-10	A-19	A-23	A-26	A-29	A-31	A-35	A-38	A-41	A-44	Mean	UCC[1]	PAAS[2]
SiO_2	69.46	78.91	77.78	76.05	75.98	74.17	75.47	72.27	80.65	77.85	81.35	82.13	76.84	66.00	62.80
Al_2O_3	8.88	2.28	5.44	7.62	4.98	6.18	7.66	6.14	3.14	6.25	4.80	4.79	5.68	15.20	18.90
CaO	3.45	1.33	1.75	1.73	1.66	1.68	1.59	2.18	0.80	1.29	0.90	0.89	1.60	4.20	1.30
Fe_2O_3*	3.47	1.03	1.89	2.47	2.48	1.78	1.57	4.47	1.38	2.12	1.42	1.59	2.14	4.50	6.50
K_2O	2.61	2.02	2.12	2.28	2.16	2.31	2.45	2.09	1.98	2.26	2.21	2.21	2.22	3.40	3.70
MgO	2.12	0.70	0.84	0.88	0.93	1.05	0.78	1.26	0.63	0.59	0.36	0.43	0.88	2.20	2.20
Na_2O	1.10	1.82	1.42	1.83	2.05	2.06	1.96	1.96	1.45	1.39	1.36	1.38	1.65	3.90	1.20
TiO_2	0.49	0.15	0.24	0.31	0.29	0.24	0.21	0.54	0.16	0.27	0.17	0.18	0.27	0.50	1.00
P_2O_5	0.13	0.05	0.09	0.07	0.09	0.05	0.05	0.09	0.04	0.06	0.04	0.09	0.07	0.17	0.16
Elements ($\times10^{-6}$)															
Mn	500	156	379	384	449	302	290	1031	206	438	266	406	400.6	-	-
Ba	314	153	183	259	215	215	249	200	167	223	216	209	216.9	550.0	650.0
Rb	134	91	99	101	90	98	103	79	84	96	97	94	97.2	112.0	160.0
Sr	124	101	107	178	153	182	194	173	115	142	131	127	143.9	350.0	200.0
V	55	5	20	32	26	21	19	65	9	26	9	13	25.0	60.0	150.0
Zr	207	90	117	132	144	98	105	280	91	126	94	93	131.4	190.0	210.0
Hf	3	3	3	3	3	3	3	3	3	3	3	3	3.0	5.8	5.0
Sc	6	1	3	4	3	3	1	7	0	2	0	0	2.5	11.0	16.0
Th	30	28	33	34	30	31	34	32	31	36	34	34	32.3	10.7	14.6
U	2	2	2	2	2	2	2	2	2	2	2	2	2.0	2.8	3.1
Ni	25	59	101	87	57	56	59	41	45	89	89	72	65.0	20.0	55.0
Co	6	1	2	2	4	2	1	8	0	3	1	1	2.6	10.0	23.0
Pb	18	19	19	18	18	18	19	16	19	19	19	20	18.5	20.0	20.0
Cr	702	1080	1347	1285	1491	944	807	852	1043	1252	1273	1252	1110.7	35.0	110.0
Y	25	23	25	23	24	24	24	25	23	25	24	24	24.1	22.0	27.0
F	456	227	130	219	191	64	29	166	78	23	49	5	136.4	-	-
Cl	53	51	47	54	46	46	48	40	38	121	38	40	51.8	-	-
Gd	4	2	3	3	3	3	3	5	3	4	3	3	3.3	3.8	4.7
Cs	4	4	5	4	4	4	5	3	4	5	5	5	4.3	-	-
Nb	15	15	17	13	15	16	17	13	16	18	17	18	15.8	25.0	19.0
La	8	9	5	1	10	8	1	59	6	16	4	8	11.3	30.0	38.0
Zn	34	11	2	4	1	3	8	6	2	5	8	39	10.3	-	-
Mo	3	9	16	8	1	10	17	18	14	19	22	23	13.3	-	-
La/Sc	1.3	9.0	1.7	0.3	3.3	2.7	1.0	8.4	-	8.0	-	-	-	2.7	2.4
Sc/Th	0.2	0.0	0.1	0.1	0.1	0.1	0.0	0.2	-	0.1	-	-	-	1.0	1.1
Co/Th	0.2	0.0	0.1	0.1	0.1	0.1	0.0	0.3	-	0.1	0.0	0.0	-	0.9	1.6
Cr/Th	23.4	38.6	40.8	37.8	49.7	30.5	23.7	26.6	33.6	34.8	37.4	36.8	-	3.3	7.5
La/Co	1.3	9.0	2.5	0.5	2.5	4.0	1.0	7.4	-	5.3	4.0	8.0	-	3.0	1.7
Mn*	0.20	0.22	0.34	0.23	0.30	0.27	0.31	0.40	0.21	0.36	0.31	0.45	0.3	-	-
V/(V+Ni)	0.69	0.08	0.17	0.27	0.31	0.27	0.24	0.61	0.17	0.23	0.09	0.15	0.27	-	-
V/Cr	0.08	0.00	0.01	0.02	0.02	0.02	0.02	0.08	0.01	0.02	0.01	0.01	0.03	-	-
U/Th	0.07	0.07	0.06	0.06	0.07	0.06	0.06	0.06	0.06	0.06	0.06	0.06	0.06	-	-
Ni/Co	4.17	59.00	50.50	43.50	14.25	28.00	59.00	5.13	-	29.67	89.00	72.00	41.29	-	-
CIA*	57.30	23.87	42.99	48.14	37.78	41.76	47.54	40.87	35.37	48.17	44.50	45.41	42.8	57	75
PIA*	74.11	7.97	53.88	61.59	45.19	52.07	60.67	51.40	35.42	61.61	55.14	56.54	51.3	59	86
W*	55.53	8.31	22.61	25.50	22.15	17.18	15.96	37.57	18.00	26.76	18.32	22.28	24.2	25.5	71.8
ICV	1.49	3.09	1.52	1.25	1.92	1.47	1.12	2.03	2.04	1.27	1.34	1.39	1.7	1.3	0.8

Notes: Total iron as Fe^2O^{3*}, UCC[1]= Upper Continental Crust and PAAS[2]=Post-Archean Australian Shale (Taylor and McLennan, 1985; Condie, 1993). CIA*=100×[Al_2O_3/(Al_2O_3+CaO*+Na_2O+K_2O)], PIA* = [(Al_2O_3 - K_2O)/(Al_2O_3 + CaO* + Na_2O - K_2O)]×100, W=0.203×ln(SiO_2)+0.191×ln(TiO_2)+0.296×ln(Al_2O_3)+0.215×ln($Fe_2O_3^*$)−0.002×ln(MgO)−0.448×ln(CaO*)−0.464×ln(Na_2O)+0.008×ln(K_2O)−1.374, there CaO* represents the CaO in the silicate fraction only (Fedo et al., 1995). ICV=[$Fe_2O_3^*$+K_2O+Na_2O+CaO+MgO+TiO_2/Al_2O_3], Mn* = log[(Mn_{sample}/Mn_{shales})/(Fe_{sample}/Fe_{shales})].

4 Results

Compositions of major and trace elements of the Holocene borehole sediments from Alamdanga, Chuadanga district, Bangladesh are presented in Table 1.

4.1 Major and trace elements

The overall chemical compositions of the sediments, in accordance with stratigraphy, exhibit relatively wide variations, especially SiO_2 from 69.46 (sample A-01) to 82.13 wt% (sample A-44), with an average of 76.84 wt% and Al_2O_3 from 2.28 wt% to 8.88 wt%, with an average of 5.68 wt% (Table 1). Stratigraphically SiO_2 variations display continuous increasing trends with increasing depth. Moreover, SiO_2 is higher than the mean value for the Upper Continental Crust (UCC) in the studied sediments (Taylor and McLennan, 1985; McLennan, 2001; Rudnick and Gao, 2003). The behavior of most of the major oxides (e.g. Al_2O_3, MgO, CaO, K_2O, TiO_2, P_2O_5 and Fe_2O_3) show strong linear negative trends with SiO_2 and only Na_2O denotes scattered distribution due to outlier of few data (Fig. 2a).

However, K_2O, Fe_2O_3, MgO, CaO and TiO_2 exhibit positive correlations with Al_2O_3 (Fig. 2b) suggesting major influences of hydraulic fractionation (Roy and Roser, 2012). In this study, amount of CaO percentage is comparatively high with wide range (0.80 wt%–3.45 wt%), which indicates the presence of plagioclase with some carbonate minerals. However, Sr shows positive correlation with Al_2O_3 (Fig. 3), which may be associated with feldspar since it is a common substitute for Ca in plagioclase. The average CaO (1.6 wt%) contents are depleted to the UCC and almost similar to that of the Post Archaean Australian Shales (PAAS) (Taylor and McLennan, 1985). The higher correlation coefficient between Al_2O_3 and K_2O (r=+0.87) suggests k-feldspar control on the major element composition of the sediments. This is also supported by the positive correlation between K_2O and Rb (Fig. 2c) with the same correlation coefficient (r=+0.87). The Na_2O contents of sediments range from 1.10 wt% to 2.06 wt%, which are depleted to the UCC and mostly similar with PASS, while K_2O contents range from 1.98 wt% to 2.61 wt%, those are slightly depleted relative to UCC and PAAS (Condie, 1993; Taylor and McLennan, 1985). Very high ratio of SiO_2/Al_2O_3 (7.8–34.6) reflects the abundance of quartz as well as the feldspar content (Potter, 1978). The ratio Na_2O/K_2O (0.42–0.95) of sediments is comparatively low, indicating the low degree of maturation of the sediments (Pettijohn et al., 1972; Roser and Korsch, 1986; Fedo et al., 1995; Paikaray et

al., 2008). The studied sediments also have lower TiO_2 (avg. 0.27 wt%) values than the UCC (Taylor and McLennan, 1985; Condie, 1993), which suggests more evolved (felsic) material in the source rocks. Most of the samples have low P_2O_5 (avg. 0.07 wt%) contents, explaining the lesser amount of accessory phases such as apatite and monazite compared with UCC (Condie, 1993).

The trace elements, especially the transition elements (Cr and Ni) have higher concentrations range of $(702-1491)\times10^{-6}$ and $(25-101)\times10^{-6}$, respectively, than UCC (Condie, 1993) and PAAS (Taylor and McLennan, 1985) values in the studied sediments but have lower concentrations of Co $(0-8\times10^{-6})$ (Table 1). Whereas, average concentrations of the large ion lithophile elements (LILE) and high field strength elements (HFSE) like Rb (avg. 97.2×10^{-6}), Ba (avg. 216.9×10^{-6}), Sr (avg. 143.9×10^{-6}), Cs (avg. 4.3×10^{-6}), Zr (avg. 131.4×10^{-6}), Hf (avg. 3×10^{-6}), Nb (avg. 15.8×10^{-6}), La (avg. 11.3×10^{-6}) and U (avg. 2×10^{-6}) of the sediments are comparatively lower than average upper crustal compositions (Taylor and McLennan, 1981), excluding the higher amount of Th (avg. 32.3×10^{-6}) and Y (avg. 24.1×10^{-6}) concentrations. Large amount of Th (32.25×10^{-6}) may indicate allanite–monazite control on REE (e.g. La, Y and Gd) (Condie et al., 1992). Some trace elements (e.g. Ba, Rb and Sr) show clear positive trend with Al_2O_3 (Fig. 3), especially Ba (r=+0.91) confirming clear hydraulic fractionation (Roy and Roser, 2012). Strong positive correlations of mobile elements suggest their association with finer particles marked hydraulic separation of quartz and clays.

In comparison to the UCC (Taylor and McLennan, 1985) the studied Holocene sediments are depleted in most of the major and trace elements (Fig. 4). The Multi-element normalized diagram exhibits enrichment only of SiO_2 and Th. These normalized elemental distributions indicates that the chemical weathering led to removal of the soluble elements from the clastic fractions compared to the insoluble hydrolysates (Nagarajan et al., 2013). These comparative depletion or enrichment of various elements is widely applicable for provenance characteristics and weathering conditions (Etemad-Saeed et al., 2011).

5 Discussion

5.1 Geochemical classifications

Although the geochemical classification of sediments is not well developed, various authors have proposed few classification schemes for clastic sedimentary rocks or sediments based on their geochemical compositions (e.g. Pettijohn et al., 1972; Herron, 1988;
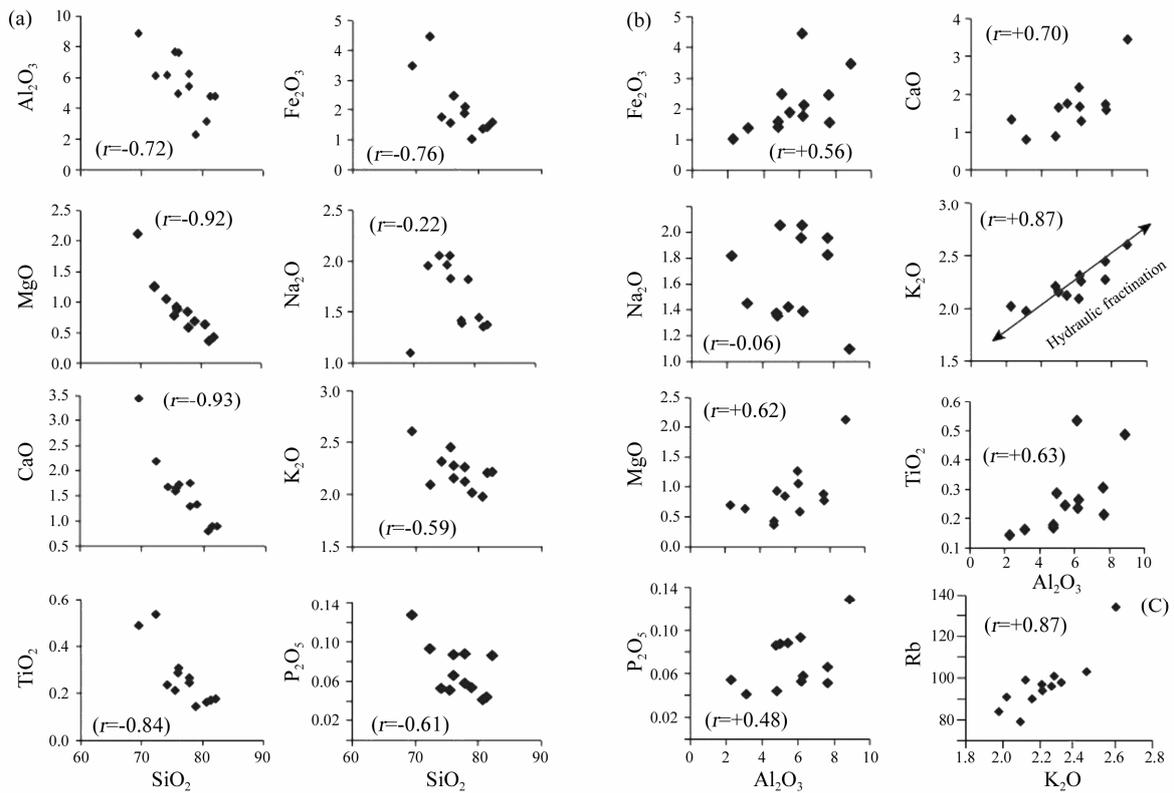
Fig. 2. Harker major element variation (in wt%) diagrams for the investigated sediments from the Bengal Basin. (a) Plots of SiO_2 vs. different oxides; (b) plots of Al_2O_3 vs. different oxides; and (c) plot of K_2O vs. Rb.
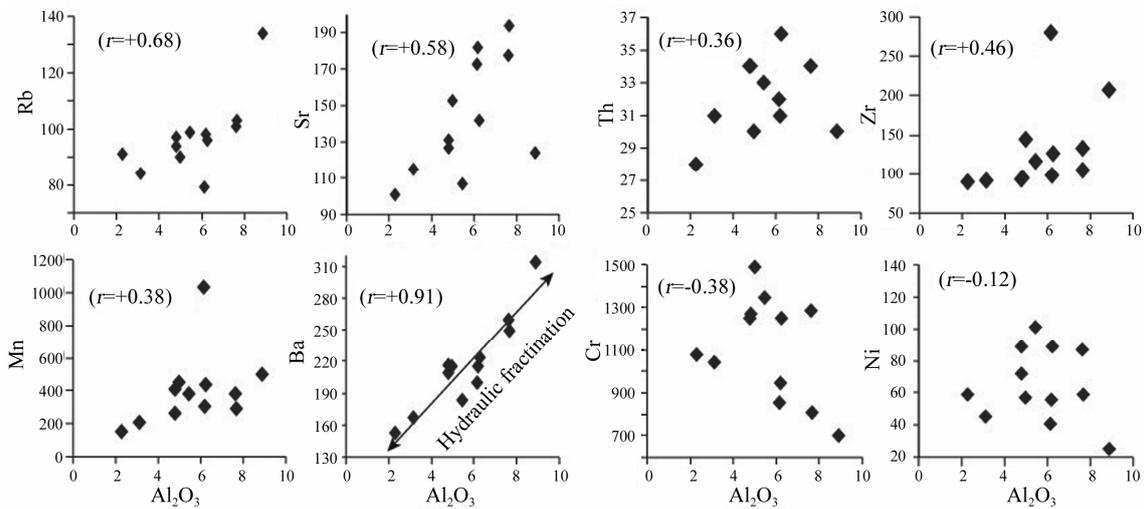

Fig. 3. Harker trace element variations (in $\times 10^{-6}$) diagrams for the investigated sediments.

Blatt et al., 1980; Crook, 1974). The SiO_2 content and the SiO_2/Al_2O_3 ratio are the most commonly used geochemical criteria for delineating the sediment maturity (Potter, 1978), which also reflect the abundance of quartz, feldspar and clay contents in the sediments. Even the alkali content ($Na_2O + K_2O$) is very much applicable for index of chemical maturity and also a measure of the feldspar content. Using an index of chemical maturity and the Na_2O/K_2O ratio, Pettijohn

et al. (1972) proposed a classification for terrigenous sedimentary rocks based upon a plot of log (Na_2O/K_2O) vs. log (SiO_2/Al_2O_3). Based on this scheme the investigated sediments show mostly sub-arkose with few sub-litharenite (Fig. 5). However, the classification scheme log (Fe_2O_3/K_2O) vs. log (SiO_2/Al_2O_3) which is the modification of Pettijohn et al. (1972) diagram by Herron (1988) provides consistent sub-arkose and arkose with considerable amount

of sub-litharenite and litharenite (Figure not shown). It is very remarkable that (Fe₂O₃* + MgO)-Na₂O-K₂O ternary diagram (Blatt et al., 1980) also displays uniform arkosic distributions of the investigated sediments (Fig. 6). Whereas, applicability of the Na₂O-K₂O diagram (Fig. 10a) for the investigated sediments, it is well enough to observe their quartz-rich characteristics (Crook, 1974).
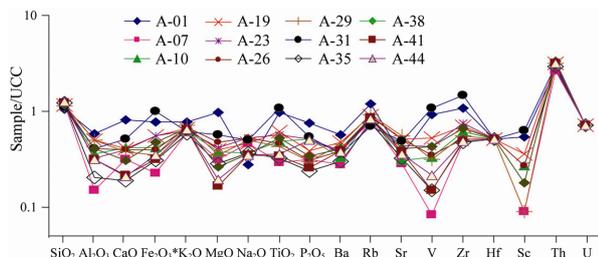

Fig. 4. Multi-element normalized diagram for the investigated sediments, normalized against average upper continental crust (Taylor and McLennan, 1985).
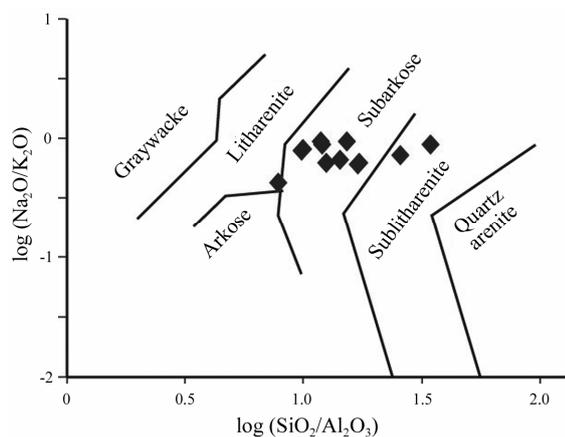

Fig. 5. Plot of the investigated Holocene sediments on geochemical classification diagrams; log (Na₂O/K₂O) vs. log (SiO₂/Al₂O₃) (after Pettijohn et al., 1972).
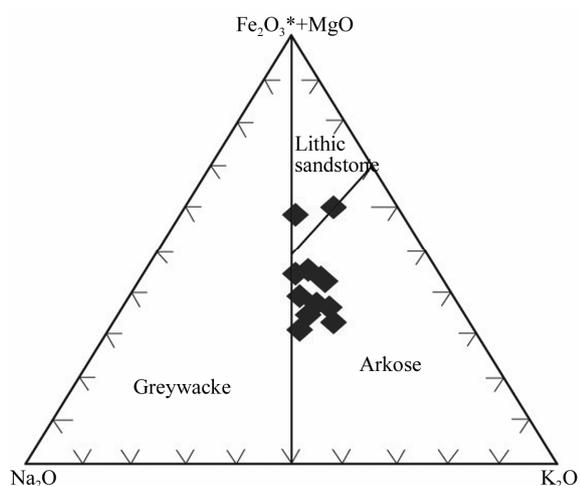
Fig. 6. (Fe₂O₃*+MgO)−Na₂O−K₂O classification diagram for the sediments from Chuadanga, Bangladesh (Blatt et al., 1980).

5.2 Source area weathering

A variety of geological issues, including the regulation of long-term climate, the release of nutrients into the biosphere and the control of primary sediment yield derived from rock decomposition, control the system of material recycling upon the Earth's surface due to the prime mechanism of weathering processes (Ohta and Arai, 2007). Identification of mechanism of weathering processes, degree of weathering or various chemical weathering indices are very useful tools in characterizing and determining the extent of weathering. The degree of chemical weathering of the source area materials can be constrained by calculating the chemical index of alteration (CIA) (Nesbitt and Young, 1982). Whereas, Ohta and Arai (2007) proposed the W index, which is very sensitive to chemical changes that occur during weathering processes. This index is more significant as it used more oxides (eight major oxides) and its applicability to a wide range of felsic, intermediate and mafic igneous rock types, whereas most conventional indices are defined by between two and four oxides. These ternary diagrams (Fig. 7a, b) infer, especially, that M and F vertices indicate mafic and felsic rock source, respectively, while the W vertex identifies the degree of weathering of the sources, independent of the chemistry of the unweathered parent rock (Ohta and Arai, 2007). The calculated data of the studied sediments display near F vertex, which suggest poor weathering as similar as unweathered igneous suite like the granitic weathering profile, where it also shows a compositional linear trend extending from the F vertex to the W vertex. In the profile (Fig. 7b), the bulk density decreases with increasing intensity of weathering (Rudnick et al., 2004). While W* index (8.31–55.53, avg. 24.2) also suggests poor weathering trend except top layer of sediments (sample A-01, Table 1). The calculated CIA* values range from 23.87 to 57.30 (avg. 42.81) in the investigated sediments (Table 1). Most of the sediment samples have CIA* values lower than 50, which imply poor weathering conditions in the source area of the sediments. These results also support by plagioclase index of alteration (PIA*) (7.97–74.11, avg. 51.3) and Index of Compositional Variability (ICV) (1.12–3.09, avg. 1.7) values (Nesbitt and Young, 1982; Fedo et al., 1995; Cox et al., 1995).

On the Al₂O₃ – (CaO* + Na₂O) – K₂O (A-CN-K) molecular proportion diagram (Fig. 7c) of Nesbitt and Young (1982), the analyzed samples plot very close to the plagioclase and K-feldspar tie lines, suggesting very poor weathering conditions or albitic-rich sources with less K mobility. The degrees of weathering for the sediment samples are fairly different throughout the sequence (Fig. 7c), indicating non-

steady-state weathering conditions (Nesbitt et al., 1997) in the source area probably due to increases in the intensity of tectonic activity throughout some periods of time at least, which permits rapid erosion of source rocks. The K_2O/Na_2O ratios are >1 suggesting quartz enrichment in the sediments and the major elements, especially the high content of SiO_2 (69.46 wt%– 82.13 wt%) also reflect quartz dominance in sediments. Variation in Al_2O_3 content (2.28 wt%–8.88 wt%) indicates feldspar input rather than clay minerals that are almost absent in the samples. In this case most

of the weathering indices suggest poor weathering. Besides, the Rb/Sr ratios of sediments also monitor the degree of source-rock weathering (McLennan et al., 1993). The Rb/Sr ratios of the studied sediments are in the range of 0.46 to 1.08 (avg. 0.71); these values are very higher than the average upper continental crust (0.32), rather near to the average PAAS (0.80; McLennan et al., 1993). All these suggest that the degree of source area weathering was most probably poor rather than moderate (Asiedu et al., 2000).
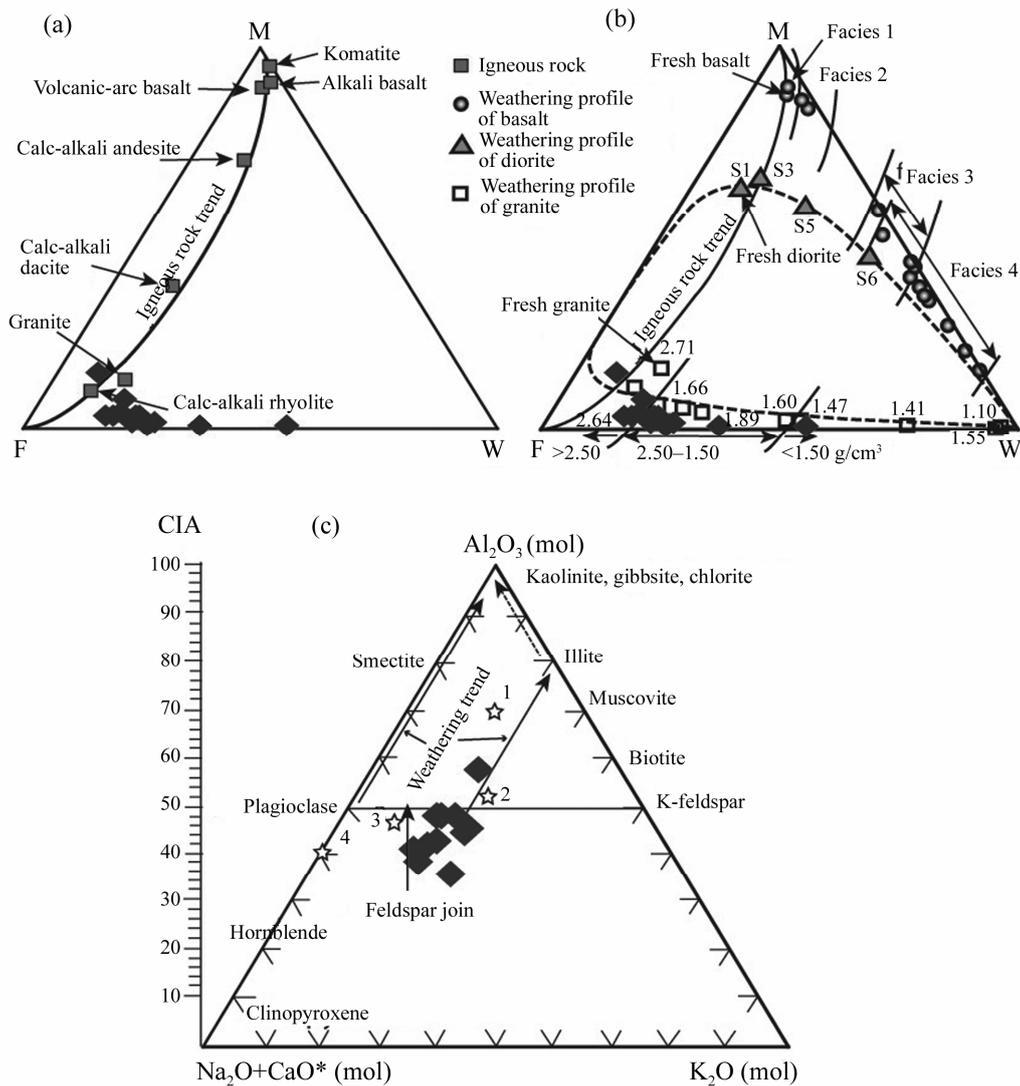

Fig. 7. Triangular diagrams for source area weathering. (a) the MFW plots for representative igneous rocks and (b) weathering profiles (Ohta and Arai, 2007). The line in (a) represents a compositional linear trend for igneous rocks. The broken lines in (b) are compositional linear trends for weathering profiles of basalt, diorite and granite. Samples from the basalt profile are classified into the following facies: fresh (facies 1), intermediately weathered (facies 2), extensively weathered (facies 3) to soil (facies 4). In the diorite profile, the proportions of secondary weathering minerals increase in the following order: S1, S3, S5 to S6. The numbers along the granite weathering profile indicate the bulk densities of the samples, which provide an estimate of the degree of weathering. Note that a decrease in the bulk density generally corresponds with an increase in the W value (Ohta and Arai, 2007); (c) Al_2O_3–(CaO*+ Na_2O)–K_2O (A–CN–K) diagram for the investigated sediments (compositions as molar proportions, CaO* represents CaO of the silicate fraction only). Selected rock and mineral compositions and weathering trends (after Nesbitt and Young, 1982) are given with open star, average N-MORB (1, Sun and McDonough, 1989) and average granite (2, Nockolds, 1954) as well as average upper continental crust (3), and average post-Archean Australian shale (4) (after Taylor and McLennan, 1985) are shown for comparison.

5.3 Sorting and sediment recycling

Sorting generates geochemical contrasts among sand, silt and clay due to separation of these grains by hydraulic fractionation and the degree of sorting is controlled by the source to sink distance, energy of the transport system, and many other factors (Dokuz and Tanyolu, 2006, Roy and Roser, 2012). The evaluation of sorting effects and their degrees by Harker variation diagrams are so much helpful on such sediments. The major oxides versus Al_2O_3 plots (Fig. 2b) exhibit poor linear trends, except K_2O (r=+0.87) and CaO (r=+0.70) showing considerable positive trends explaining the extent of fractionation through mineral sorting. The ICV of the studied Holocene sediments are more than 1 (1.12–3.09), suggesting that they are compositionally immature to moderately mature and were likely dominated by first cycle input (Cullers and Podkovyrov, 2000). Al_2O_3-TiO_2-Zr ternary diagram (Fig. 8) (Garcia et al., 1994) implies the influence of sorting processes and provides information on the zircon concentration in sediments with a limited range of TiO_2-Zr, indicating low compositional maturity and insignificant sorting of the sediments. It is noted that the studied sediments support a limited range of TiO_2-Zr variation and a clear sorting trend, and those consisting of sand-size components are immature suggesting poor to moderate sorting and deposition without recycling. With an increase in SiO_2/Al_2O_3 (7.8–34.6) ratio the grain size also increases, as do the extent of recycling and maturity of sediment. The good correlations between CIA and other elements, such as CIA–Al_2O_3 (r=+0.88), suggest that grain-size and sorting were played significant roles in determining the CIA values. Hence, the depleted CIA values and good correlation between CIA and Al_2O_3 imply poor to moderate recycling because the number of recycling increases, the degree of weathering increases. Another trace-element diagram of Th/Sc vs. Zr/Sc (not shown) is also applicable to discriminate compositional variation, degree of sediment recycling, and heavy-mineral sorting (McLennan et al., 1993). The samples display clearly a positive linear trend between the Th/Sc and Zr/Sc ratios, which expresses the igneous differentiation trend. It is also remarkable that the Th/Sc ratio of the sediments mostly higher than one (>1), suggesting continental signature. However, these illustrations are not enough to explain the size of effect of sorting. The Th/U ratio may be more applicable for understanding the influence of sorting on the compositional variation of sediments. Generally Th/U ratio in most upper crustal rocks is typically between 3.5 and 4.0 and weathering and sedimentary recycling typically result in loss of U, leading to an elevation in the Th/U ratio (McLennan et

al., 1993). In this case the ratios of Th/U (14–18) in the Holocene sediments are very higher than upper crustal rocks, indicating elevated influence of sediment recycling.
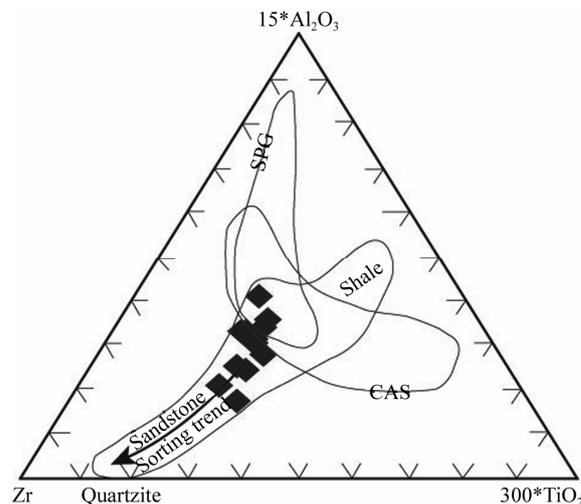

Fig. 8. Ternary plot of 15*Al_2O_3–Zr–300*TiO_2 for the investigated sediments, CAS, field of calc-alkaline granites; SPG, field of strongly peraluminous granites (after Garcia et al., 1994).

5.4 Climate and redox conditions

The degree of chemical weathering is a function of climate and rates of tectonic uplift (Wronkiewicz and Condie, 1987). The raising chemical weathering intensity suggests the decrease in tectonic activity and/or the change of climate towards warm and humid conditions which are more favorable for chemical weathering in the source region (Jacobson et al., 2003). The Holocene sediments of the study area reflect low weathering conditions from CIA[*], PIA[*] and W[*] index (Table 1). Low CIA[*] (avg. 42.81), PIA[*] (avg. 51.30) and high ICV (>1) values in the investigated sediments indicate the near absence of chemical alteration and might reflect cool and/or arid climate conditions (Fedo et al., 1995; Etemad-Saeed et al., 2011). Whereas, the applicability of the ratios of $SiO_2/(Al_2O_3+K_2O+Na_2O)$ for paleoclimatic condition (Suttner and Dutta, 1986) during deposition of the sediments in the basin is well recognized by many workers. The plot SiO_2 vs. $(Al_2O_3+K_2O+Na_2O)$ (Fig. 9) displays reasonable semi-arid to semi-humid climatic conditions in the area. It is noted that during Holocene (~3–12 ka, Stanley and Hait, 2000) period the area was under comparatively humid climatic condition, which reflecting comparable results after Last Glacial Maxima (LGM) conditions in this region.

Redox condition is very important for recognizing the sediment deposition in marine or non-marine environments. Moreover, the accumulation of certain

trace metals in sediments is directly or indirectly controlled by redox conditions through either a change in redox state and/or speciation (McKay et al., 2007). In this case, the Mn* value is a significant paleochemical indicator of the redox conditions of the depositional environment (Bellanca et al., 1996; Cullers, 2002; Machhour et al., 1994). For calculating Mn^* value, the applicable basic formula is $Mn^*=log[(Mn_{sample}/Mn_{shales})/(Fe_{sample}/Fe_{shales})]$, where the values used for the Mn_{shales} and Fe_{shales} are $600{\times}10^{-6}$ and $46150{\times}10^{-6}$, respectively (Wedepohl, 1978). The reduced iron and manganese form different solubilities of compounds across a redox boundary, while manganese tends to accumulate in more oxygenated conditions above the redox boundary (Bellanca et al., 1996). Thus, the present sediments have the positive Mn* values (0.2–0.45, avg. +0.301), suggesting that these sediments may have been deposited in oxic and/or nearly suboxic conditions. Moreover, the investigated sediments also show significant fluctuations/variations in V (5–65)$\times10^{-6}$ and Ni (25–101)$\times10^{-6}$ content throughout the sequence. The vanadium solubility in natural waters, its extraction from seawater and absorption onto sediments are mainly influenced by redox conditions (Bellanca et al., 1996). During the early diagenetic alteration of sediments, V tends to mobilize from the biogenic materials under oxic environments, whereas the mobilization of V is very restricted in anoxic conditions (Shaw et al., 1990). Moreover, Ni is mainly enriched in organic-rich sediments where these metals are trapped with organic matter (Leventhal and Hosterman, 1982; Gilkson et al., 1985). The proportionality of these two elements V/(V+Ni) is very significant to delineate information on Eh, pH and sulphide activity in the depositional environment (Madhavaraju and Lee, 2009 and references therein). Nevertheless, V accumulates relative to Ni in reducing environments, where sulphate reduction is more efficient. The Holocene sediments show low V/(V+Ni) ratios (0.08–0.69, avg. 0.27), only two samples (A-01 and A-31) have higher values. The V/(V+Ni) ratios of these sediments are mostly similar to those of normal marine marginal systems (Lewan, 1984). The V/(V+Ni) ratios are lower than 0.8, which indicates the moderate frequency in the redox state of the depositional environment. The Ni/Co ratio is also a redox indicator (Nagarajan et al., 2007; Dypvik, 1984; Dill, 1986). Jones and Manning (1994) proposed that Ni/Co ratios below 5 indicate oxic environments, whereas ratios above 5 suggest suboxic and anoxic environments. The Holocene sediments show high Ni/Co ratio (0–89; only two samples provide <5) which suggest that these sediments were deposited suboxic and anoxic environments. However, anoxic and suboxic sediments are enriched in Mo (Nameroff et al., 2002), this statements only support lower part of

the sediments (samples A-38, A-41, A-44). The investigated Holocene sediments occasionally exhibit few typical signature of oxidation (brownish gray and light brown colors), but they do not consist of hardened (stiff) muds with calcareous and/or iron concretions. These results suggest that the investigated sediments deposited in mostly oxic deltaic conditions (G-B delta) during Holocene, at ~3–12 ka (Stanley and Hait, 2000).
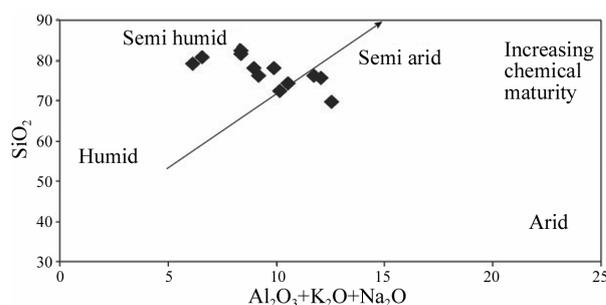

Fig. 9. Bivariate plot of SiO_2 vs. ($Al_2O_3 + K_2O + Na_2O$) to discriminate paleoclimatic condition during the deposition of the Holocene sediments (after Suttner and Dutta, 1986).

5.5 Provenance

Geochemical data and their various approaches are very significant for relevant provenance demarcation (Keskin, 2011; Armstrong-Altrin et al., 2004; Taylor and McLennan, 1985; Cullers, 1995; Condie et al., 1992). Major elements provide information on both the rock composition of the provenance and the effects of sedimentary processes, such as weathering and sorting (McLennan et al., 1993). These also explain the characteristics of the source rocks and finally provide definite styles of sedimentary history (Dickinson, 1985, 1988). It is very remarkable that the ratios of SiO_2/Al_2O_3 (7.8–34.6) and K_2O/Na_2O (1.1–2.4) of the studied sediments are higher than those ratios of UCC (Taylor and McLennan, 1985; Condie, 1993), reflecting that the investigated sediments were derived largely from crustal granitic sources. The Al_2O_3/TiO_2 ratio of the investigated sediments ranges from 11.5 to 35.8. Such higher Al_2O_3/TiO_2 values (avg. 22.49) are suggested to be derived from mostly felsic to intermediate rock sources (Hayashi et al., 1997; Keskin, 2011 and references therein). The bivariate plot of Na_2O-K_2O (Crook, 1974; Fig. 10a) provides quartz-rich nature of the sediments. Another triangular plot of $(CaO+MgO)$-$SiO_2/10$-(Na_2O+K_2O) (not shown) represent most remarkable and precise picture of the provenance, which shows clear distance from the fields of ultramafites and basalts, but close to the field of granites, indicating dominance of felsic contribution (after Taylor and McLennan, 1985). Discrimination function diagram (Fig. 10b) for the provenance

signatures of the sediments using major elements (Roser and Korsch, 1988) refers to quartzose sedimentary provenance, comparable fields with the Tertiary sedimentary rocks in Bangladesh (Hossain et al., 2010; Roy and Roser, 2012) and Siwalik, India (Ranjan and Banerjee, 2009), however the studied Holocene sediments maintain clear distance from both the Tertiary sedimentary rocks and Siwalik deposits. The investigated Holocene sediments contain comparatively high K_2O and Rb concentrations and their K/Rb ratios of 161–219 lie close to the main trend with a ratio of 230 of a typical differentiated magmatic suite (Fig. 11a) proposed by Shaw (1968). These results highlight the chemically coherent nature of the sediments and derivation mainly from acidic to intermediate rocks. Moreover, the concentration of zircon is used to characterizing the nature and composition of source rock (Hayashi et al., 1997; Paikaray et al., 2008). The low TiO_2/Zr ratios (16 to 24) of the sediments indicate felsic source rocks (Keskin, 2011 and references therein). Hayashi, et al. (1997) stated that the TiO_2/Zr ratios are so much supportive to distinguish among three different source rock types, i.e., felsic, intermediate and mafic. Based on Hayashi, et al. (1997), the TiO_2 versus Zr plot (Fig. 11b) of the investigated sediments characterize felsic source rocks.

Although felsic source rocks contain comparatively low Cr, Ni, Co and V, some heavy mineral concentrations make uncertainty, e.g. Cr (702×10^{-6}–1491×10^{-6}) concentration of sediments are very high possibly due to the high concentrations of chromian spinel, chromite and magnetite or significant ophiolitic component (Nagarajan et al., 2013). Generally those trace elements are useful indicators of mafic and ultramafic source (Wornkiewicz and Condie, 1987; Huntsman-Mapila et al., 2005). The investigated sediments contain lower concentrations of Co (0–$8)\times10^{-6}$, and V (5–$65)\times10^{-6}$ than mafic and intermediate source rocks (Taylor and McLennan, 1985; Wronkiewicz and Condie, 1987; Spalletti et al., 2008) and moderate concentrations of Ba (153–$314)\times10^{-6}$, Sr (101–$194)\times10^{-6}$, Ni (25–$101)\times10^{-6}$, Y (23–$25)\times10^{-6}$ and Zr (90–$280)\times10^{-6}$. The Cr/Zr ratio is expected to decrease if zircons are concentrated by hydraulic sorting in the sedimentary process (Taylor and McLennan, 1985; Spalletti et al., 2008). The investigated sediments show a broad range of Cr/Zr ratios (3.04–13.54), which is very much identical to the value of the originating from a mafic to felsic sources. The value of Y/Ni ratios (0.25–1.0) is identical to the value of the sediments from the felsic source, which is also supported from the moderate Th/Sc and Zr/Sc ratios, respectively. La and Y show significantly scatter correlation with Zr suggesting a minor influence of zircon and other REE-rich heavy minerals, probably because it is controlled largely by irregular distribu-

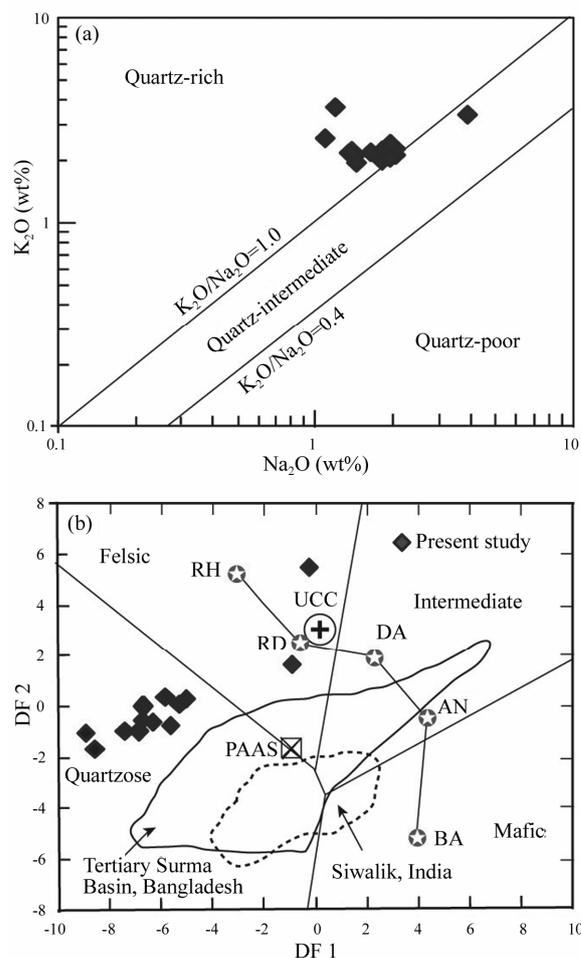tion during sedimentation (Lopez et al., 2005).

Fig. 10. (a) Plot of Na_2O versus K_2O of the Holocene sediments from Chuadanga, Bangladesh showing quartz-rich nature (Crook, 1974), and (b) major element provenance discriminant plot (Roser and Korsch, 1988), where fields for Siwalik, India from data in Ranjan and Banerjee (2009), Tertiary sedimentary rocks, Surma Basin from Hossain et al. (2010), Hatia trough from Roy and Roser (2012), UCC and PAAS from Taylor and McLennan (1985). Stars. BA, AN, DA, RD, RH—average basalt, andesite, dacite, rhyodacite and rhyolite, as plotted by Roser and Korsch (1988).

5.6 Tectonic setting

Sedimentary rocks from different tectonic settings have varying geochemical characteristics (Bhatia, 1983; Roser and Korsch, 1986). Major and trace-elements and their various bivariate and multivariate plots with discrimination functions are mostly applicable for tectonic setting of the sedimentary basins. Although these applications are not always valid for specific local plate-tectonic settings such as back-arc basin, some correlations between tectonic settings and geochemical composition of sediments could be established and the relationships among

temporal and spatial variations within various lithostratigraphic units, can be evaluated. The plot of (K_2O/Na_2O) vs. SiO_2 (Fig. 12a) provides a tectonic setting discrimination for the investigated sediments (Roser and Korsch, 1986), showing passive margin (PM) with few active continental margin (ACM) tectonic setting. The discrimination function diagram (Fig. 12b) for tectonic setting also provides comparable result with PM and few samples offer continental island arc (CIA) signatures. This is reliable with the definition of passive margin which includes sedimentary basins on trailing continental margins supplied from collisional orogens (Najman, 2006). Bhatia and Crook (1986) also believed that La/Sc vs. Ti/Zr diagram is the most useful trace element tectonic discrimination plot (not shown), which displays that the sediments are mostly concentrated within or near the PM and CIA fields, confirming the intimacy of the major element analysis. Some trace element concentrations (e.g. Ba, Rb, Pb and Y) and the ratios of Ti/Zr (9.7–14.4), La/Sc (0.3–9.0) also indicate clearly passive margin (PM) tectonic setting (Bhatia and Crook, 1986).

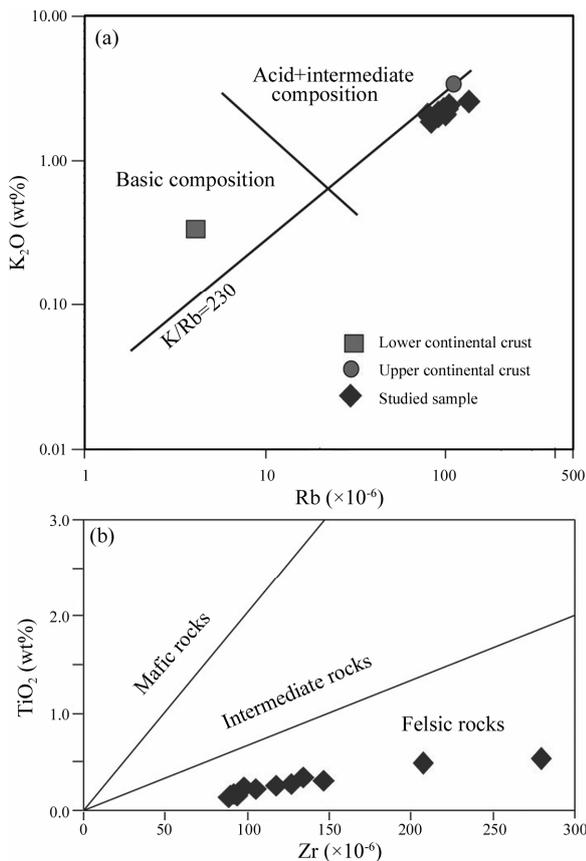Fig. 11. (a) Bivariate plot of K_2O vs. Rb of the Holocene sediments relative to a K/Rb ratio of 230 (main trend of Shaw, 1968). Average Upper and Lower Continental Crust data from Taylor and McLennan (1985); (b) TiO_2-Zr plot for the Holocene sediments from Chuadanga, Bangladesh (Hayashi et al., 1997).
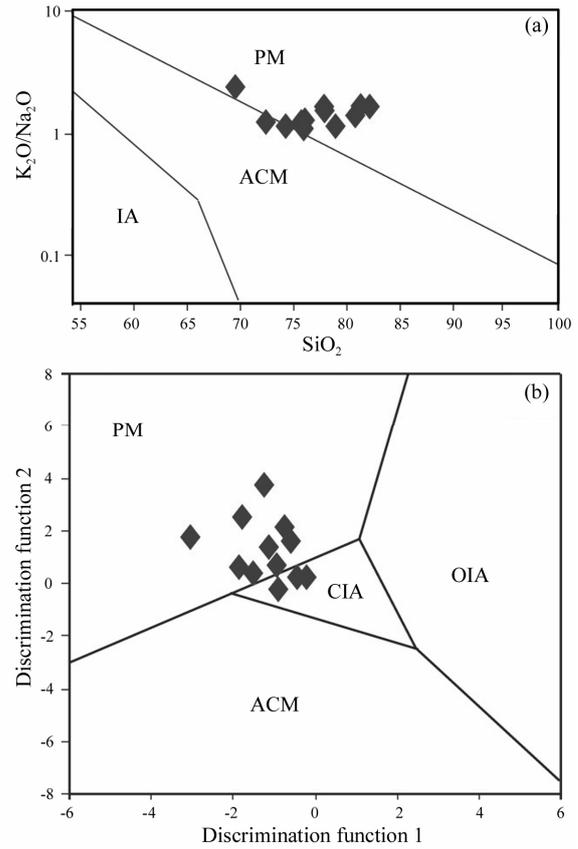

Fig. 12. (a) Tectonic setting discrimination diagram of SiO_2 vs. log (K_2O/Na_2O) for the investigated Holocene sediments (after Roser and Korsch, 1986); (b) the discriminant function diagram for the investigated sediments (after Bhatia, 1983), where PM = passive margin, ACM = active continental margin, IA = island arc, CIA = continental island arc, OIA = oceanic island arc.

6 Summary and conclusions

Clastic sediments contain important information about the composition, tectonic setting and evolution of continental crust. Their chemical records are affected by factors such as source rock characteristics, climate, chemical weathering and sorting processes during transportation, sedimentation and post-depositional diagenesis. The Holocene sediments from Chuadanga area show mostly wider variations in their major element geochemistry, reflecting the non-steady-state conditions for provenance and tectonic setting. Geochemical classification of the sediments shows mainly sub-arkose with few sub-litharenite. Some major and trace elements show apparent positive correlation with Al_2O_3 confirming clear hydraulic fractionation. The ratio of SiO_2/Al_2O_3 (7.8–34.6), W* index (8.31–55.53), CIA* values (23.87–57.30), ICV (>1) and PIA* values (7.97–74.11) show low degrees of maturity and indicating poor chemical weathering in source areas. Whole rock geochemistry data suggest mainly felsic to intermediate provenance types. These

types of source rocks are present in a vast region of the Himalayan belt and catchment areas of Ganges. Discrimination diagrams show the continental signature derivatives, which are chiefly consisted of quartzose sedimentary provenance, comparable fields with the Tertiary sedimentary rocks in Bangladesh and Siwalik, India. Therefore, the sediments might have been derived from the felsic to intermediate igneous rocks as well as from quartzose sedimentary/metamorphic provenance. The low CIA* values as well as the low Th/Sc ratio (Cullers, 2000) suggest that the source rock for the sediments might be formed a mixed old continental source, composed mostly of granitic and, to a very lesser extent, mafic rocks. Sediment samples have high abundance of Cr and high ratios of Th/Sc were most likely to be contributed from a mafic provenance, like Cr-spinel rich ophiolite source from Himalayan Suture Zone. The considerably high CaO of the sediments suggest that these were derived from plagioclase rich intermediate rocks with some contributions from a few carbonate rocks. Due to the positive Mn* values, the sediments suggest their depositions mostly in oxic deltaic depositional conditions (G-B delta) during Holocene, at ~3–12 ka. The lower V/(V+Ni) and high Ni/Co ratios also indicate the moderate frequency in the redox state of the depositional environment. The tectonic setting of the sediments demarcates typically passive margin based on major and trace elements discrimination.

References

Allison M.A. (1998) Historical changes in the Ganges-Brahmaputra delta front [J]. *Journal of Coastal Research*. **14**, 1269–1275.

Allison M.A., Khan S.R., Goodbred Jr. S.L., and Kuehl S.A. (2003) Stratigraphic evolution of the late Holocene Ganges–Brahmaputra lower delta plain [J]. *Sedimentary Geology*. **155**, 317–342.

Allison M.A., Kuehl S.A., Martin T.C., and Hassan A. (1998) The importance of floodplain sedimentation for river sediment budgets and terrigenous input to the oceans: Insights from the Brahmaputra–Jamuna River [J]. *Geology*. **26**, 175–178.

Armstrong-Altrin J.S., Lee Y.I., Verma S.P., and Ramasamy S. (2004) Geochemistry of sandstones from the Upper Miocene Kudankulam Formation, southern India: Implications for provenance, weathering, and tectonic setting [J]. *Journal of Sedimentary Research*. **74**, 285–297.

Asiedu D.K., Suzuki S., Nogami K., and Shibata T. (2000) Geochemistry of Lower Cretaceous sediments, Inner Zone of Southwest Japan: Constraints on provenance and tectonic environment [J]. *Geochemical Journal*. **34**, 155–173.

Basu A. (1985) Influence of climatic and relief on compositions of sands released at source areas. In *Provenance of Arenites: NATO, Advanced Study Institute Series* (ed. Zuffa G.G.). [M]. pp.1–18.

Bellanca A., Claps M., Erba E., Masetti D., Neri R., Premolisilva I., and Venezia F. (1996) Orbitally induced limestone/marlstone rhythms in the Albian-Cenomanian Cismon section (Venetian region, northern Italy): Sedimentology, calcareous and siliceous plankton distribution, elemental and isotope geochemistry [J]. *Paleogeography, Paleoclimatology and Paleoecology*. **126**, 227–260.

Bhatia M.R. (1983) Plate tectonics and geochemical composition of sandstones [J]. *Journal of Geology*. **92**, 181–193.

Bhatia M.R. and Crook K.A.W. (1986) Trace element characteristics of graywackes and tectonic setting discrimination of sedimentary basin [J]. *Contributions to Mineralogy and Petrology*. **92**, 181–193.

Blatt H., Middleton G., and Murray R. (1980) *Origin of Sedimentary Rocks* [M]. pp.782. 2nd edition, Prentice-Hall, New Jersey.

Condie K.C. (1993) Chemical composition and evolution of the upper continental crust: Contrasting results from surface samples and shales [J]. *Chemical Geology*. **104**, 1–37.

Condie K.C., Noll P.D., and Conway C.M. (1992) Geochemical and detrital mode evidence for two sources of Early Proterozoic metasedimentary rocks from the Tonto Basin Supergroup, central Arizona [J]. *Sedimentary Geology*. **77**, 51–76.

Cox R., Low D.R., and Cullers R.L. (1995) The influence of sediment recycling and basement composition on evolution of mudrock chemistry in the southwestern United States [J]. *Geochimica et Cosmochimica Acta*. **59**, 2919–2940.

Crook K.A.W. (1974) Lithogenesis and geotectonics: The significance of compositional variation in flysch arenites (greywackes) [J]. *Society of Economical, Paleontological and Mineralogical Special Publications*. **19**, 304–310.

Cullers R.L. (1995) The controls on the major and trace element evolution of shales, siltstones and sandstones of Ordovician to Tertiary age in the Wet Mountain region, Colorado, U.S.A. [J]. *Chemical Geology*. **123**, 107–131.

Cullers R.L. (2000) The geochemistry of shales, siltstones and sandstones of Pennsylvanian-Permian age, Colorado, USA: Implications for provenance and metamorphic studies [J]. *Lithos*. **51**, 181–203.

Cullers R.L. (2002) Implications of elemental concentrations for provenanace, redox conditions, and metamorphic studies of shales and limestones near Pueblo, Co, USA [J]. *Chemical Geology*. **191**, 305–327.

Cullers R.L. and Podkovyrov V.N. (2000) Geochemistry of the Mesoproterozoic Lakhanda shales in southeastern Yakutia, Russia: Implications for mineralogical and provenance control, and recycling [J]. *Precambrian Research*. **104**, 77–93.

Curray J.R. and Moore D.G. (1971) Growth of the Bengal deep-sea fan and denudation in the Himalayas [J]. *GSA Bulletin*. **82**, 563–572.

Dalai T.K., Rengarajan R., and Patel P.P. (2004) Sediment geochemistry of the Yamuna River System in the Himalaya: Implications to weathering and transport [J]. *Geochemical Journal*. **38**, 441–453.

Dickinson W.R. (1985) Interpreting provenance relations from detrital modes of sandstones. In *Provenance of Arenites* (ed. Zuffa G.G.) [M]. pp.333–361. Dordrecht-Boston-Lancaster. D. Reidel Pub. Co.

Dickinson W.R. (1988) Provenance and sediment dispersal in relation to

paleo-tectonics, and paleo-geography of sedimentary basins In *New Perspectives in Basin Analysis* (eds. Kleinspehn K.L. and Paola C.) [M]. pp.3–25. New Springer Verlag.

Dickinson W.R., Beard L.S., Brakenridge G.R., Erjavec J.L., Ferguson R.C., Inman K.F., Knepp R.A., Lindberg F.A., and Ryberg P.T. (1983) Provenance of North American Phanerozoic sandstones in relation to tectonic setting [J]. *Geological Society of America Bulletin.* **94**, 222–235.

Dill H. (1986) Metallogenesis of early Paleozoic graptolite shales from the Graefenthal Horst (northern Bavaria-Federal Republic of Germany) [J]. *Economic Geology.* **81**, 889–903.

Dokuz A. and Tanyolu E. (2006) Geochemical constraints on the provenance, mineral sorting and subaerial weathering of Lower Jurassic and Upper Cretaceous clastic rocks of the eastern Pontides, Yusufeli (Artvin), NE Turkey [J]. *Turkish Journal of Earth Sciences.* **15**, 181–209.

Dypvik H. (1984) Geochemical compositions and depositional conditions of Upper Jurassic and Lower Cretaceous Yorkshire clays, England [J]. *Geological Magazine.* **121**, 489–504.

Etemad-Saeed N., Hosseini-Barzi M., and Armstrong-Altrin J.S. (2011) Petrography and geochemistry of clastic sedimentary rocks as evidences for provenance of the Lower Cambrian Lalun Formation, Posht-e-Badam block, Central Iran [J]. *Journal of African Earth Sciences.* **61**, 142–159.

Fedo C.M., Nesbitt H.W., and Young G.M. (1995) Unraveling the effects of potassium metasomatism in sedimentary rock sand paleosols, with implications for paleoweathering conditions and provenance [J]. *Geology.* **23**, 921–924.

Garcia D., Fonteilles M., and Moutte J. (1994) Sedimentary fractionation between Al, Ti, and Zr and genesis of strongly peraluminous granites [J]. *Journal of Geology.* **102**, 411–422.

Gilkson M., Chappell B.W., Freeman R.S., and Webber E. (1985) Trace elements in oil shales, their source and organic association with particular reference to Australian deposits [J]. *Chemical Geology.* **53**, 155–174.

Goto A. and Tatsumi Y. (1994) Quantitative analysis of rock samples by an X-ray fluorescence spectrometer (I) [J]. *The Rigaku Journal.* **11**, 40–59.

Goto A. and Tatsumi Y. (1996) Quantitative analysis of rock samples by an X-ray fluorescence spectrometer (II) [J]. *The Rigaku Journal.* **13**, 20–38.

Hayashi K., Fujisawa H., Holland H.D., and Ohmoto H. (1997) Geochemistry of 1.9 Ga sedimentary rocks from northeastern Labrador, Canada [J]. *Geochimica et Cosmochimica Acta.* **61**, 4115–4137.

Herron M.M. (1988) Geochemical classification of terrigeneous sands and shales from core or log data [J]. *Journal of Sedimentary Petrology.* **58**, 820–829.

Hossain H.M.Z., Roser B.P., and Kimura J.I. (2010) Petrography and whole-rock geochemistry of the Tertiary Sylhet succession, northeastern Bengal Basin, Bangladesh: Provenance and source area weathering [J]. *Sedimentary Geology.* **228**, 171–183.

Huntsman-Mapila P., Kampunzu A.B., Vink B., and Ringrose S. (2005) Cryptic indicators of provenance from the geochemistry of the Okavango Delta sediments, Bostwana [J]. *Sedimentary Geology.* **174**, 123–148.

Jacobson A.D., Blum J.D., Chamberlian C.P., Craw D., and Koons P.O. (2003) Climate and tectonic controls on chemical weathering in the New Zealand Southern Alps [J]. *Geochimica et Cosmochimica Acta.* **37**, 29–46.

Jones B. and Manning D.C. (1994) Comparison of geochemical indices used for the interpretation of paleo-redox conditions in ancient mudstones [J]. *Chemical Geology.* **111**, 111–129.

Johnsson M.J. (1993) The system controlling the composition of clastic sediments [J]. *Geological Society of America* (Special Paper). **284**, 1–19.

Keskin S. (2011) Geochemistry of Çamardı Formation sediments, central Anatolia (Turkey): Implication of source area weathering, provenance, and tectonic setting [J]. *Geosciences Journal.* **15**, 185–195.

Khan F.H. (1991) *Geology of Bangladesh* [M]. pp.207. Willey Eastern limited, New Delhi, India.

Leventhal J.S. and Hosterman J.W. (1982) Chemical and mineralogical analysis of Devonian black-shale samples from Martin County, Kentucky; Carroll and Washington counties, Ohio; Wise County, Virginia; and Overton County, Tennessee, U.S.A. [J]. *Chemical Geology.* **37**, 239–264.

Lewan M.D. (1984) Factors controlling the proportionality of vanadium to nickel in crude oils [J]. *Geochimica et Cosmochimica Acta.* **48**, 2231–2238.

Lopez J.M.G., Bauluz B., Fernandez-Nieto C., and Oliete A.Y. (2005) Factors controlling the trace-element distribution in fine-grained rocks: The Albian kaolinite-rich deposits of the Oliete Basin (NE Spain) [J]. *Chemical Geology.* **214**, 1–19.

Machhour L., Philip J., and Oudin J.L. (1994) Formation of laminate deposits in anaerobic-dysaerobic marine environments [J]. *Marine Geology.* **117**, 287–302.

Madhavaraju J. and Lee Y.I. (2009) Geochemistry of the Dalmiapuram Formation of the Uttatur Group (Early Cretaceous), Cauvery Basin, southeastern India: Implications on provenance and paleo-redox conditions [J]. *Revista Mexicana de Ciencias Geológicas.* **26**, 380–394.

McKay J.L., Pedersen T.F., and Mucci A. (2007) Sedimentary redox conditions in continental margin sediments (N.E. Pacific)—Influence on the accumulation of redox-sensitive trace metals [J]. *Chemical Geology.* **238**, 180–196.

McLennan S.M. (1993) Weathering and global denudation [J]. *Journal of Geology.* **101**, 295–303.

McLennan S.M. (2001) Relationships between the trace element composition of sedimentary rocks and upper continental crust [J]. *Geochemistry Geophysics Geosystems.* **2**, 2000GC000109.

McLennan S.M., Hemming S., McDaniel D.K., and Hanson G.N. (1993) Geochemical approaches to sedimentation, provenance and tectonics [J]. *Geological Society of America* (Special Paper). **285**, 21–40.

Milliman J.D. and Syvitski P.M. (1992) Geomorphic/Tectonic control of sediment discharge to the ocean: The importance of small mountainous rivers [J]. *Journal of Geology.* **100**, 524–544.

Nagarajan R., Madhavaraju J., Nagendra R., Armstrong-Altrin J.S., and Moutte J. (2007) Geochemistry of Neoproterozoic shales of the Rabanpalli Formation, Bhima Basin, northern Karnataka, southern India: Implications for provenance and paleoredox conditions [J]. *Revista Mexicana de Ciencias Geológicas.* **24**, 150–160.

Nagarajana R., Roy P.D., Jonathan M.P., Lozano R., Kessler F.L., and Prasanna M.V. (2013) Geochemistry of Neogene sedimentary rocks from Borneo Basin, East Malaysia: Paleo-weathering, provenance and tectonic setting [J]. *Chemie Der Erde-Geochemistry.*

http://dx.doi.org/10.1016/j.chemer.2013.04.003.

Najman Y. (2006) The detrital record of orogenesis: A review of approaches and techniques used in the Himalayan sedimentary basins [J]. *Earth-Science Reviews*. **74**, 1–72.

Najman Y., Bickle M., BouDagher-Fadel M., Carter A., Garzanti E., Paul M., Wijbrans J., Willett E., Oliver G., Parrish R., Akhter S.H., Allen R., Ando S., Chisty E., Reisberg L., and Vezzoli G. (2008) The Paleogene record of Himalayan erosion: Bengal Basin, Bangladesh [J]. *Earth and Planetary Science Letters*. **273**, 1–14.

Nameroff T.J., Balistrieri L.S., and Murray J.W. (2002) Suboxic trace metal geochemistry in the eastern tropical North Pacific [J]. *Geochimica et Cosmochimica Acta*. **66**, 1139–1158.

Nesbitt H.W., Fedo C.M., and Young G.G. (1997) Quartz and feldspar stability, steady and non-steady-state weathering, and petrogenesis of siliciclastic sands and muds [J]. *Journal of Geology*. **105**, 173–191.

Nesbitt H.W. and Young G.M. (1982) Early Proterozoic climates of sandstone mudstone suites using SiO_2 content and K_2O/Na_2O ratio [J]. *Nature*. **299**, 715–717.

Nockolds S.R. (1954) Average chemical compositions of some igneous rocks [J]. *Geological Society of America, Bulletin*. **65**, 1007–1032.

Ohta T. and Arai H. (2007) Statistical empirical index of chemical weathering in igneous rocks: A new tool for evaluating the degree of weathering [J]. *Chemical Geology*. **240**, 280–297.

Paikaray S., Banerjee S., and Mukherji S. (2008) Geochemistry of shales from Paleoproterozoic to Neoprotzoic Vindhyan Super-group: Implications on provenance, tectonic and paleoweathering [J]. *Journal of Asia Earth Science*. **32**, 34–48.

Pate R.D., Goodbred S.L. Jr., and Khan S.R. (2009) Delta Double-Stack: Juxtaposed Holocene and Pleistocene Sequences from the Bengal Basin, Bangladesh [J]. *The Sedimentary Record*. **7**, 4–9.

Pettijohn F.J., Potter P.E., and Siever R. (1972) Sand and Sandstone. Plate motions inferred from major element chemistry of lutites [J]. *Precambrian Research*. **147**, 124–147.

Potter P.E. (1978) Petrology and chemistry of big river sands [J]. *Journal of Geology*. **86**, 423–449.

Ranjan N. and Banerjee D.M. (2009) Central Himalayan crystallines as the primary source for the sandstone-mudstone suites of the Siwalik Group: New geochemical evidence [J]. *Gondwana Research*. **16**, 687–696.

Raymo M.E. and Ruddiman W.F. (1992) Tectonic forcing of Late Cenozoic climate [J]. *Nature*. **359**, 117–122.

Roser B.P. and Korsch R.J. (1986) Determination of tectonic setting of sandstone mudstone suites using SiO_2 content and K_2O/Na_2O ration [J]. *Journal of Geology*. **94**, 635–650.

Roser B.P. and Korsch R.J. (1988) Provenance signatures of sandstone-mudstone suites determined using discriminant function analysis of major-element data [J]. *Chemical Geology*. **67**, 119–139.

Roy D. and Roser B.P. (2012) Geochemistry of the Tertiary sequence in the Shahbajpur-1 well, Hatia Trough, Bengal Basin, Bangladesh: Provenance, source weathering and province affinity [J]. *Journal of Life and Earth Science*. **7**, 1–13.

Rudnick R.L. and Gao S. (2003) Composition of the continental crust. In

The Crust Treatise on Geochemistry (ed. Rudnick R.L.) [M]. Elsevier-Pergamon, Oxford.

Rudnick R.L., Tomascak P.B., Njo H.B., and Gardner L.R. (2004) Extreme lithium isotopic fractionation during continental weathering revealed in saprolites from South Carolina [J]. *Chemical Geology*. **212**, 45–57.

Sarkar A., Sengupta S., McArthur J.M., Ravenscroft P., Bera M.K., Bhushan R., Samanta A., and Agrawal S. (2009) Evolution of Ganges–Brahmaputra western delta plain: Clues from sedimentology and carbon isotopes [J]. *Quaternary Science Reviews*. **28**, 2564–2581.

Shaw D.M. (1968) A review of K-Rb fractionation trends by covariance analysis [J]. *Geochimica et Cosmochimica Acta*. **32**, 573–602.

Shaw T.J., Geiskes J.M., and Jahnke R.A. (1990) Early diagenesis in differing depositional environments: The response of transition metals in pore water [J]. *Geochimica et Cosmochimica Acta*. **54**, 1233–1246.

Sinha S., Islam R., Ghosh S.K., Kumar R., and Sangode S.J. (2007) Geochemistry of Neogene Siwalik mudstones along Punjab re-entrant, India: Implications for source-area weathering, provenance and tectonic setting [J]. *Current Science*. **92**, 1103–1113.

Spalletti L.A., Queralt I., Matheos S.D., Colombo F., and Maggi J. (2008) Sedimentary petrology and geochemistry of siliciclastic rocks from the Upper Jurassic Tordillo Formation (Neuquen Basin, western Argentina): Implications for provenance and tectonic setting [J]. *Journal of South American Earth Sciences*. **25**, 440–463.

Stanley D.J. and Hait A.K. (2000) Holocene depositional patterns, neotectonics and sundarbon mangroves in the western Ganges-Brahmaputra Delta [J]. *Journal of Coastal Research*. **16**, 26–39.

Sun S.S. and Mcdonough W.F. (1989) Chemical and isotopic systematics of oceanic basalts: Implications for mantle composition and processes. In: (eds. Saunders A.D. and Norry M.J.) *Magmatism in the Ocean Basins*. [J]. *Geological Society of London, Special Publication*. **42**, 315–345.

Suttner L.J. and Dutta P.K. (1986) Alluvial sandstone composition and paleoclimate 1. Framework mineralogy [J]. *Journal of Sedimentary Petrology*. **56**, 326–345.

Taylor S.R. and McLennan S.M. (1981) The composition and evolution of the continental crust: Rare earth evidence from sedimentary rocks [J]. *Philosophical Transactions of the Royal Society of London Series A—Mathematical Physical and Engineering Sciences*. **30**, 381–399.

Taylor S.R., and McLennan S.M. (1985) *The Continental Crust: Its Composition and Evolution. An Examination of the Geochemical Record Preserved in Sedimentary Rocks* [M]. pp.312. Blackwell Science, Oxford.

Uddin A. and Lundberg N. (2004) Miocene sedimentation and subsidence during continent-continent collision, Bengal Basin, Bangladesh [J]. *Sedimentary Geology*. **164**, 131–146.

Wedepohl K.H. (1978) *Manganese: Abundance in Common Sediments and Sedimentary Rocks* [M]. pp.1−17. Handbook of Geochemistry: Springer Berlin.

Wronkiewicz D.J. and Condie K.C. (1987) Geochemistry of Archean shales from the Witwatersrand Supergroup, South Africa: Source-area weathering and provenance [J]. *Geochimica et Cosmochimica Acta*. **51**, 2401–2416.